JACS
JOURNAL OF THE AMERICAN CHEMICAL SOCIETY

Article

pubs.acs.org/JACS

Robust and Porous β-Diketiminate-Functionalized Metal–Organic Frameworks for Earth-Abundant-Metal-Catalyzed C–H Amination and Hydrogenation

Nathan C. Thacker, Zekai Lin, Teng Zhang, James C. Gilhula, Carter W. Abney, and Wenbin Lin*

Department of Chemistry, University of Chicago, 929 East 57th Street, Chicago, Illinois 60637, United States

Supporting Information

ABSTRACT: We have designed a strategy for postsynthesis installation of the β-diketiminate (NacNac) functionality in a metal–organic framework (MOF) of UiO-topology. Metalation of the NacNac-MOF (**I**) with earth-abundant metal salts afforded the desired MOF-supported NacNac-M complexes (M = Fe, Cu, and Co) with coordination environments established by detailed EXAFS studies. The NacNac-Fe-MOF catalyst, **I**•Fe(Me), efficiently catalyzed the challenging intramolecular sp^3 C–H amination of a series of alkyl azides to afford α-substituted pyrrolidines. The NacNac-Cu-MOF catalyst, **I**•Cu(THF), was effective in promoting the intermolecular sp^3 C–H amination of cyclohexene using unprotected anilines to provide access to secondary amines in excellent selectivity. Finally, the NacNac-Co-MOF catalyst, **I**•Co(H), was used to catalyze alkene hydrogenation with turnover numbers (TONs) as high as 700 000. All of the NacNac-M-MOF catalysts were more effective than their analogous homogeneous catalysts and could be recycled and reused without a noticeable decrease in yield. The NacNac-MOFs thus provide a novel platform for engineering recyclable earth-abundant-element-based single-site solid catalysts for many important organic transformations.

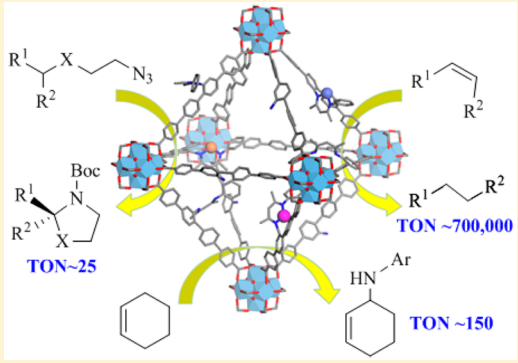

INTRODUCTION

The inherent toxicity and scarcity of precious metals have fueled intense research efforts to develop replacements using earth-abundant elements, i.e., base metals, to catalyze known and new organic transformations. Significant progress has recently been made using homogeneous base metal catalysts to effect such sustainable catalytic reactions.[1] The design of homogeneous base metal catalysts often requires bulky substituents proximal to the active site to prevent intermolecular catalyst deactivation. However, these sterically protective ligands often require multiple-step synthesis elaboration and attenuate the catalytic activity of base metal catalysts, both of which adversely impact the practicality of many earth-abundant metal catalysts.[2] Alternative strategies are sorely needed to allow homogeneous base metal catalysts to develop from novel discoveries into practical applications.

Immobilizing homogeneous precious metal catalysts on porous solid supports such as mesoporous silicas has been extensively explored with the goal of recycling and reusing valuable catalysts.[3] However, such a strategy can lead to nonuniform distribution of catalysts and cannot completely prevent intermolecular interactions between catalytic sites or interactions of active sites with surface functionalities. The difficulty of characterizing nonuniformly distributed heterogeneous catalysts presents another significant challenge. To this end, we have recently initiated research efforts to design earth-abundant metal catalysts using metal–organic frameworks (MOFs).[4]

MOFs are an emerging class of crystalline, porous molecular materials with potential for application in many areas, such as catalysis,[5−7] drug delivery,[8] nonlinear optics,[9] sequestration/separation,[10] and gas storage.[11] The versatility of MOFs comes from their high degree of tunability, i.e., the shapes and dimensionalities of their channels and pores may be modulated by varying the length and substitution patterns of their organic linkers, whereas incorporation of orthogonal functional groups on the organic linkers offers a reliable synthesis handle for subsequent functionalization. In particular, Zr-based MOFs of UiO-topology with $Zr_6(\mu_3\text{-}O)_4(\mu_3\text{-}OH)_4$ secondary building units (SBUs) and linear dicarboxylate linkers have provided an ideal platform for designing efficient MOF catalysts because of their stability in a broad range of solvents and under harsh reaction conditions.[12] We report here the postsynthesis installation of the β-diketiminate functionality in a UiO-type MOF.

β-Diketiminate ligands, commonly called NacNac, are a useful class of bidentate ligands with the propensity to coordinate to a wide variety of metals.[13] Their modular synthesis allows for both steric and electronic tuning of the ligand. Functionalization within a MOF gives access to low coordinate metal complexes without the need of steric bulk to protect the metal active site. We show in this paper that the coordination of Fe(II) and Cu(I) centers with postsynthesis-

Received: December 22, 2015
Published: February 17, 2016

DOI: 10.1021/jacs.5b13394
J. Am. Chem. Soc. 2016, 138, 3501–3509

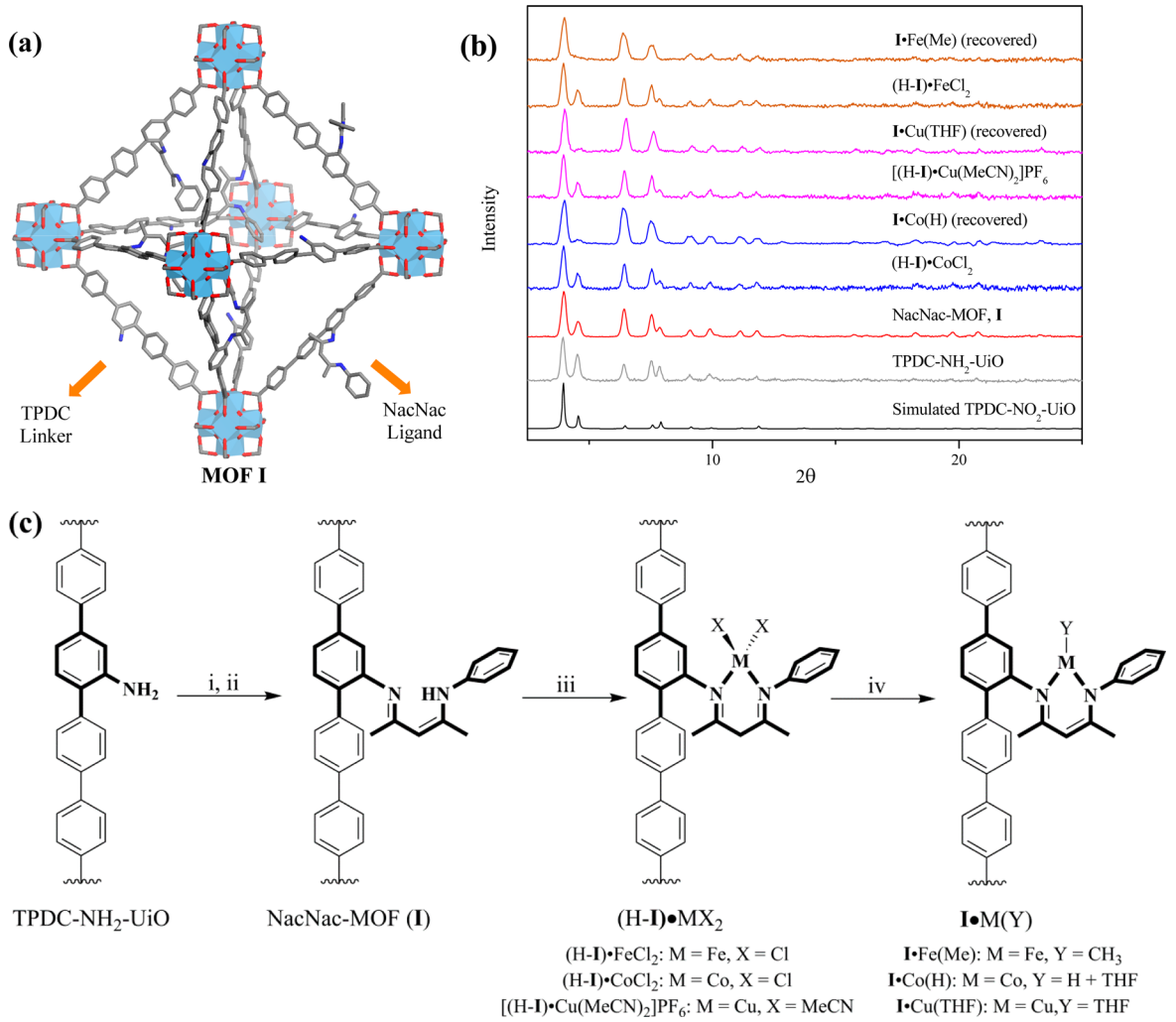

Figure 1. (a) Structural model showing the octahedral cage of NacNac-functionalized MOF **I**. (b) PXRD patterns of various MOF samples: TPDC-NO_2-UiO simulated from the CIF file (black), TPDC-NH_2-UiO (gray), NacNac-MOF **I** (red), (H–**I**)•$CoCl_2$ (blue), **I**•Co(H) recovered from catalysis (blue), [(H–**I**)•$Cu(MeCN)_2$]PF_6 (pink), **I**•Cu(THF) recovered from catalysis (pink), (H–**I**)•$FeCl_2$ (brown), and **I**•Fe(Me) recovered from catalysis (brown) (c) Synthesis sequence showing NacNac installation and metalation: (i) Et_3OBF_4 (1.1 equiv of w.r.t. amino ligand), 4-*N*-phenylamino-3-penten-2-one (1.1 equiv of w.r.t. amino ligand), DCM. (ii) KOtBu (0.7 equiv of w.r.t. amino ligand). (iii) $FeCl_2$·$4H_2O$ (0.75 equiv of w.r.t. amino ligand), $CoCl_2$ (0.75 equiv of w.r.t. amino ligand), or $Cu(MeCN)_4PF_6$ (0.6 equiv of w.r.t. amino ligand) in THF. (iv) $NaBHEt_3$ (10 equiv of w.r.t. Fe), MeLi (5 equiv of w.r.t. Co), or KOtBu (1 equiv of w.r.t. Cu).

installed NacNac ligands in a UiO-type MOF affords highly effective catalysts for the amination of unactivated sp^3 C–H bonds. Furthermore, a Co(II)-NacNac-functionalized MOF is an excellent alkene hydrogenation catalyst with turnover numbers (TONs) as high as 700 000.

RESULTS AND DISCUSSION

Synthesis and Characterization. The amino-functionalized UiO-type MOF, $Zr_6O_4(OH)_4$(TPDC-NH_2)$_6$, was prepared in 67% yield by heating a mixture of 2″-amino-[1,1′:4′,1″:4″,1‴-tetraphenyl-]-4,4‴-dicarboxylic acid (H_2TPDC-NH_2) and $ZrCl_4$ in N,N′-dimethylformamide (DMF) and trifluoroacetic acid at 90 °C for 72 h. The TPDC-NH_2 linkers were chosen to give a MOF with large, accessible channels (Figure 1a). The powder X-ray diffraction (PXRD) pattern is similar to the pattern simulated from the single-crystal structure of $Zr_6O_4(OH)_4$(TPDC-NO_2)$_6$, a UiO-type MOF that was recently reported by our research group.[6] This result suggests that $Zr_6O_4(OH)_4$(TPDC-NH_2)$_6$ adopts UiO connectivity. Nitrogen sorption measurements indicate that $Zr_6O_4(OH)_4$(TPDC-NH_2)$_6$ is highly porous, with a BET surface area of 2136 m^2/g and pore sizes of 18.8 and 21.4 Å.

$Zr_6O_4(OH)_4$(TPDC-NH_2)$_6$ was treated with alkylated enaminone followed by deprotonation of the iminium tetrafluoroborate intermediate to afford the desired NacNac-functionalized MOF (**I**). The extent of NacNac functionalization was determined by NMR studies of **I** that had been digested in a K_3PO_4 solution in a 1:1 mixture of d_6-DMSO and D_2O for over 24 h. ^1H NMR signals of the organics revealed that ∼50% of the TPDC-NH_2 groups were converted to the TPDC-NacNac groups (Supporting Information). PXRD of **I** indicates that crystallinity is maintained throughout the postsynthetic NacNac installation process (Figure 1b).

Metalation of NacNac ligands is typically achieved by treatment with an alkyl lithium followed by the addition of a metal salt. However, this procedure can deprotonate the SBUs of **I** potentially resulting in multiple catalytically active sites in the MOF. Instead, we first prepared metal complexes of the neutral NacNac ligand and then deprotonated the NacNac ligand to afford the desired metal complexes of the

DOI: 10.1021/jacs.5b13394
J. Am. Chem. Soc. 2016, 138, 3501−3509

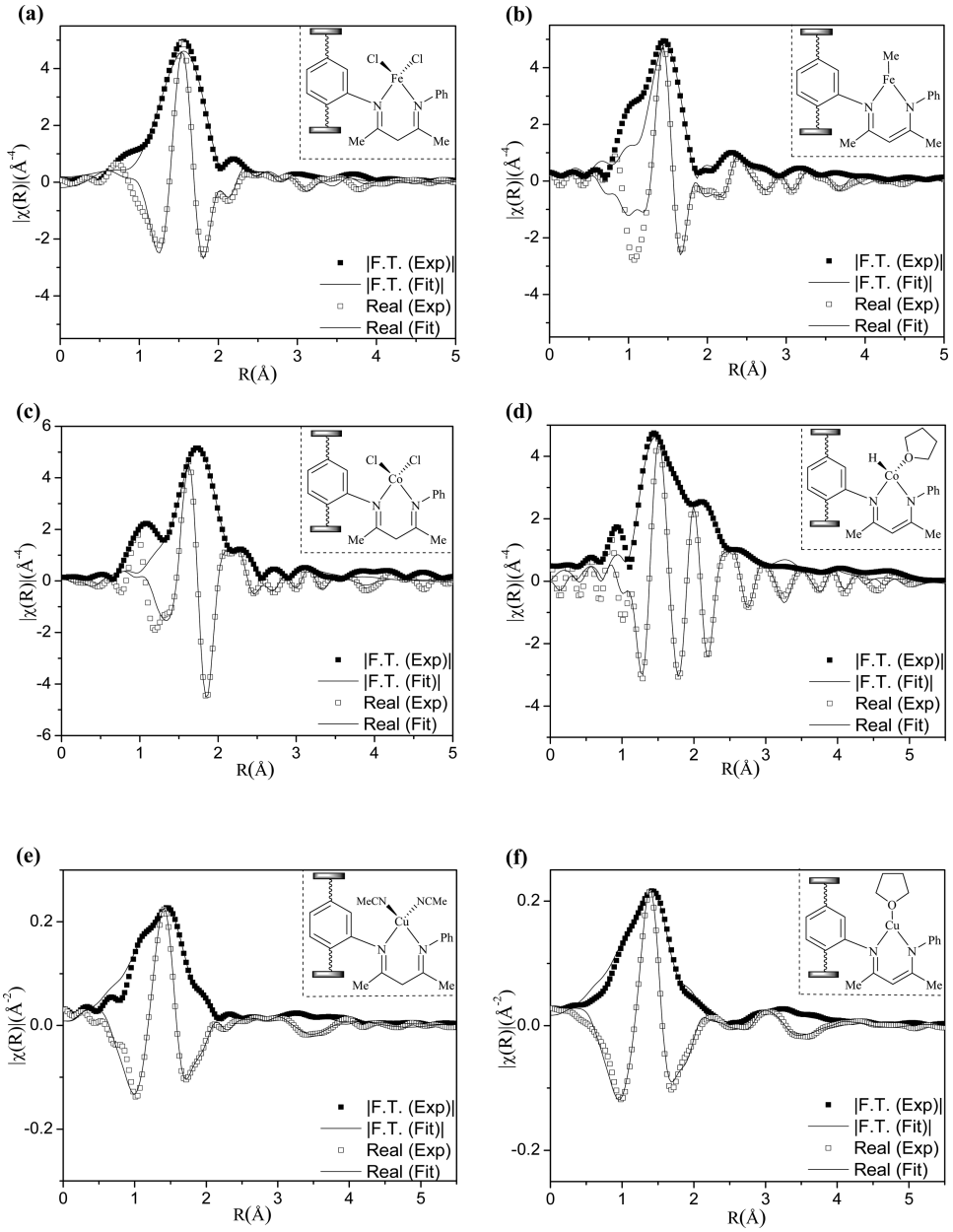

Figure 2. Extended X-ray absorption fine structure fits of metalated MOF **I** in *R*-space showing the magnitude of Fourier transform (solid squares and solid line) and real components (hollow squares and dashed line). (a) (H−**I**)•$FeCl_2$, (b) **I**•Fe(Me), (c) (H−**I**)•$CoCl_2$, (d) **I**•Co(H), (e) [(H−**I**)•$Cu(MeCN)_2$]PF_6, and (f) **I**•Cu(THF).

monoanionic NacNac ligand (Figure 1c). Solutions of $CoCl_2$, $FeCl_2$•$4H_2O$, and $[Cu(MeCN)_4]PF_6$ in THF were added to **I** to give MOF-immobilized neutral NacNac complexes (H−**I**)•$CoCl_2$, (H−**I**)•$FeCl_2$, and [(H−**I**)•$Cu(MeCN)_2$]PF_6. Inductively coupled plasma−mass spectrometry (ICP-MS) of digested metalated MOFs showed that the extents of metalation were 60, 98, and 80% for Co, Fe, and Cu (with respect to the NacNac ligand in **I**), respectively. Deprotonation and subsequent functionalization of the metals were then carried out to afford the metal complexes of the monoanionic NacNac ligand in **I**. (H−**I**)•$FeCl_2$ was treated with 5 equiv of MeLi to afford **I**•Fe(Me), whereas (H−**I**)•$CoCl_2$ was treated with 10 equiv of $NaBHEt_3$ to give **I**•Co(H). [(H−**I**)•$Cu(MeCN)_2$]PF_6 was deprotonated with addition of 1.5 equiv of KOtBu in THF to give the desired **I**•Cu(THF) species. A similar neutral metalation protocol was employed to deprotonate preformed $CoCl_2$ complexes of a family of P−N−P ligands.[14] PXRD patterns of the metalated MOF samples showed that MOFs maintain crystallinity after metalation processes.

N,N′-Ph_2-NacNac (H−**L1**) was used to prepare homogeneous controls in order to obtain the coordination environments of the M-NacNac complexes in **I** and to compare the performance of MOF catalysts with the homogeneous control catalysts. Single crystals of (H−**L1**)•$CoCl_2$ and (H−**L1**)•$FeCl_2$ were prepared from complexation of the neutral ligand with metal salts followed by crystallization in concentrated solutions of THF or diethyl ether at −10 °C, respectively (Supporting Information). Attempts to prepare complexes of (H−**L1**)•$Cu(MeCN)_2$ however failed because of immediate precipitation of amorphous powders under various conditions. For the preparation of homogeneous catalysts, precursors **L1**•FeCl

DOI: 10.1021/jacs.5b13394
J. Am. Chem. Soc. 2016, 138, 3501−3509

and **L1**•CoCl were prepared from deprotonation of (H–**L1**) followed by addition of either $FeCl_2(THF)_{1.5}$ or $CoCl_2$ in THF. These species were then treated with either MeLi or $NaBHEt_3$ to afford the active catalyst **L1**•Fe(Me) or **L1**•Co(H), respectively. Similar functionalization strategies of NacNac derivatives have been previously reported by Holland and co-workers.[15] The corresponding homogeneous **L1**•Cu catalyst was prepared by addition of CuOtBu to a solution of (H–**L1**) in benzene.

Extended X-ray Absorption Fine Structure Analysis. Extended X-ray absorption fine structure (EXAFS) analysis of the MOF samples was used to investigate the local coordination environments of the catalytically active metals. Good fits were obtained for the first and second shells surrounding the metal centers. EXAFS fitting indicates that all metal-neutral NacNac complexes within (H–**I**)•M MOFs (M = Fe, Co, and Cu) adopt tetrahedral coordination environments. The EXAFS spectrum of (H–**I**)•$FeCl_2$ was fitted with the crystal structure of (H–**L1**)•$FeCl_2$ where Fe was coordinated to one neutral NacNac ligand, with the Fe–N distance of 1.96 Å, and two chloride ligands. The EXAFS spectrum of (H–**I**)•$CoCl_2$ was fitted with the crystal structure of (H–**L1**)•$CoCl_2$ where Co was coordinated to one neutral NacNac ligand, with the Co–N distance of 2.12 Å, and two chloride ligands. The EXAFS spectrum of [(H–**I**)•$Cu(MeCN)_2$]PF_6 was fitted with a model where Cu was coordinated to one neutral NacNac ligand, with the Cu–N distance of 1.92 Å, and two acetonitrile solvent molecules. EXAFS fitting of **I**•M (M = Fe, Co, and Cu) materials indicates the formation of metal monoanionic NacNac complexes, on the basis of shorter M–N bond distances. For **I**•Fe(Me), Fe was coordinated to one monoanionic NacNac ligand, with a Fe–N distance of 1.95 Å, and one methyl group, adopting trigonal coordination environment. This type of three-coordinate Fe(NacNac)(Me) complex has been reported by Holland and co-workers.[15] For **I**•Co(H), Co was coordinated to one monoanionic NacNac ligand with a Co–N distance of 2.00 Å, one hydride ligand, and one THF solvent molecule adopting a square planar coordination environment. A small amount of Co nanoparticles (6.4%), which was presumably formed during the deprotonation process, was included to give the best fit. For **I**•Cu(THF), Cu was coordinated to one monoanionic NacNac ligand, with Cu–N distance of 1.89 Å and one THF solvent molecule, adopting a nearly trigonal coordination environment.

Catalytic Intramolecular C_{sp^3}–H Amination. Nitrogen-containing heterocycles are prevalent in bioactive pharmaceutically relevant compounds.[16] Although the construction of aryl C_{sp^2}–N bonds through traditional Buchwald–Hartwig couplings or oxidative C–H amination[17] is now well established, methodologies for constructing C_{sp^3}–N bonds are far less developed in spite of the need for sustaining high percentage of C_{sp^3}–N bonds in drug candidates to ensure their pharmacological activties.[18] Two complementary strategies may be used to install C_{sp^3}–N bonds: (1) transformation of pre-existing functional groups via classical techniques[19] such as allylic amination, reductive amination, and hydroamination or (2) direct amination of C_{sp^3}–H bonds. The latter approach requires overcoming the high C_{sp^3}–H bond energy under mild reaction conditions with chemo- and regioselectivity. We describe in this paper two elegant approaches toward C_{sp^3}–H amination by taking advantage of MOF-enabled site isolation to stabilize highly active earth-abundant metal catalysts.

Saturated N-heterocycles, in particular, are desirable in pharmaceutical compounds to minimize the possibly undesirable high aromatic ring counts.[20] For example, the α-aryl pyrrolidine motif is found in a glucokinase inhibitor (Merck)[21] and a $K_v1.5$ potassium blocker (Bristol-Myers Squibb-394136).[22] Synthesis of such N-heterocycles with α substitution has been of increasing interest.[23] One emerging strategy is direct C–H activation (Figure 3b). Betley and co-workers employed metal-based redox catalysis to effect the C_{sp^3}–H amination of 1-azido-4-phenyl-butane (**1a**) to Boc-protected α-phenyl pyrrolidine (**2a**) through a proposed Fe-nitrene intermediate.[24] Recently, van der Vlugt and co-workers reported C_{sp^3}–H amination using a Pd catalyst based on a redox-active ligand, albeit in low yields.[25] We speculated that a Fe-NacNac complex immobilized in a MOF could also be effective on the basis of the precedent from Holland and co-workers who reported that a Fe(III)-imido complex can effect H atom transfer and the catalytic nitrene transfer giving carbodiimides and isocyanates.[26] C–H functionalization with a nonheme Fe(II) complex is reminiscent of α-ketoglutarate-dependent dioxygenase catalyzing the hydroxylation of taurine through a generally accepted Fe(II) to Fe(IV) cycle.[27]

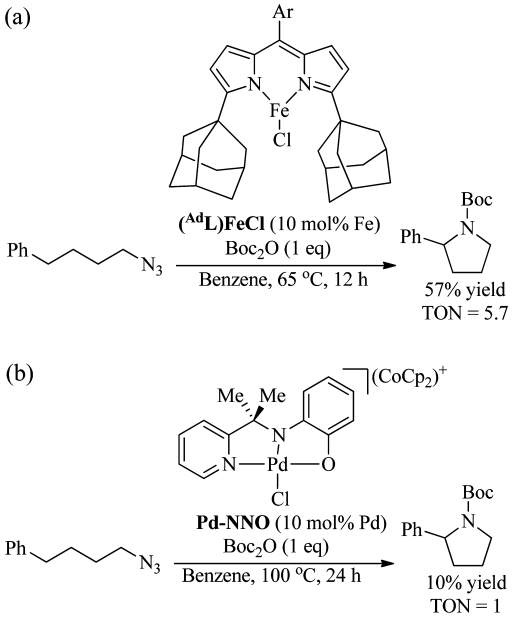

Figure 3. Intramolecular C_{sp^3}–H amination reactions catalyzed by (a) iron[24] and (b) palladium.[25]

At 5 mol % catalyst loading, homogeneous **L1**•Fe(Me) converts azide **1a** to the Boc-protected N-heterocycle **2a** in 31% yield (Table 1, entry 1). In comparison, 5 mol % of the MOF catalyst **I**•Fe(Me) (based on Fe) affords a 90% yield of **2a** (Table 1, entry 2). The increased yield of **I**•Fe(Me) relative to that of the homogeneous complex can likely be attributed to active site isolation in the MOF preventing the active catalysts from deleterious multimolecular deactivation. For example, N_2-bridged Fe(I)-NacNac complexes reductively couple adamantyl azides, giving thermally stable hexazene-bridged Fe(II) complexes in the absence of additional coordinating ligands.[28]

Varying the conditions from those previously described has an adverse effect on the reaction yield. For example, decreasing the equivalents of Boc_2O from 10 to 5 dramatically reduces the yield from 90 to 23% (Table 1, entry 1 vs 3). Betley and co-

DOI: 10.1021/jacs.5b13394
J. Am. Chem. Soc. 2016, 138, 3501–3509

Table 1. Optimization of I•Fe(Me)-Catalyzed Intramolecular C−H Amination[a]

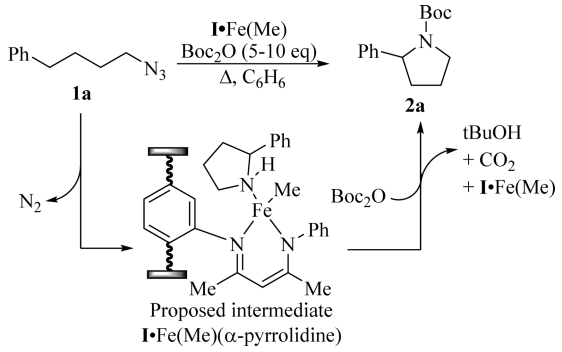

entry	catalyst (mol %)	temp. (°C)	Boc_2O (equiv)	yield **2a**[a]
1	**L1**•Fe(Me) (5)	90	10	31
2	**I**•Fe(Me) (5)	90	10	90 (83)[b]
3	**I**•Fe(Me) (5)	90	5	23
4	**I**•Fe(Me) (5)	80	10	33
5	**I**•Fe(H) (5)	90	10	>1

[a]Reaction conditions: **1a** (1 equiv), Boc_2O (5−10 equiv), catalyst at designated temperature for 48 h [b]Isolated yield.

workers proposed that Boc liberates the active catalyst from the secondary cyclic amine-Fe intermediate;[24] a larger excess of Boc protecting agent is needed in our system presumably because of its low effective concentration in MOF channels as a result of diffusional constraint. Reducing the temperature from 90 to 80 °C also resulted in a substantial drop in yield (Table 1, entry 1 vs 4). Furthermore, treating (H−**I**)•$FeCl_2$ with $NaBHEt_3$ presumably produces a **I**•Fe(H) species that gives only ∼1% conversion of the starting material.

Next, the substrate scope for the **I**•Fe(Me)-catalyzed intramolecular C_{sp^3}−H amination was explored. At 5 mol % catalyst loading, 59% yield of the desired oxazoline **2b** is obtained (Table 2, entry 3). Reducing the catalyst loading to 2 mol % and shortening the reaction time to 24 h gives the maximum TON of 25 for this substrate (Table 2, entry 4). The

Table 2. Substrate Scope for I•Fe(Me)-Catalyzed Intramolecular C−H Amination[a]

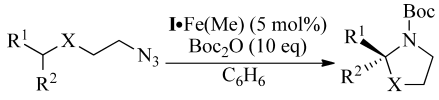

1a-1e **2a-2e**

entry	catalyst (mol %)	R1	R2	X	yield (%)
1	**I**•Fe(Me) (5)	Ph	H	CH_2	90 (**2a**)
2	**L1**•Fe(Me) (5)	Ph	H	CH_2	31 (**2a**)
3	**I**•Fe(Me) (5)	Ph	H	O	59 (**2b**)
4	**I**•Fe(Me) (2)	Ph	H	O	50 (**2b**)
5	**L1**•Fe(Me) (5)	Ph	H	O	30 (**2b**)
6	**I**•Fe(Me) (5)	Me	Me	CH_2	99 (**2c**)
7	**L1**•Fe(Me) (5)	Me	Me	CH_2	0 (**2c**)
8	**I**•Fe(Me) (5)	CH_2=CH_2	H	CH_2	65 (**2d**)
9	**I**•Fe(Me) (10)	CH_2=CH_2	H	CH_2	90 (**2d**)
10	**L1**•Fe(Me) (5)	CH_2=CH_2	H	CH_2	0 (**2d**)
11	**I**•Fe(Me) (10)	Et	H	CH_2	40 (**2e**)
12	**L1**•Fe(Me) (10)	Et	H	CH_2	0 (**2e**)

[a]Reaction conditions: **1a−1e** (1 equiv), Boc_2O (10 equiv), catalyst at 90 °C for 48 h.

homogeneous catalyst **L1**•Fe(Me) gives only 30% yield (with a TON of 6) under identical reaction conditions (Table 2, entry 5). Sterically congested substrates were tolerated well because C−H amination of 1-azido-4-methyl pentane **1c** proceeds to form gem-dimethyl N-heterocycle **2c** in quantitative yield (Table 2, entry 6). Analogous **L1**•Fe(Me) produced no conversion to the desired product (Table 2, entry 7). Reactive functional groups were tolerated as well; alkene-tagged substrate **1c** afforded cyclized product **2c** in 65% yield at 5 mol % catalyst loading (Table 2, entry 8). The yield improves to 90% by increasing the catalyst loading to 10 mol % (Table 2, entry 9). Once more, the homogeneous complex was inactive for this transformation (Table 2, entry 10). The proposed mechanism for Fe-catalyzed amination reaction involves a C−H abstraction step; thus, substrates bearing stronger C−H bonds are expected to be less effective for the amination reactions. Satisfactorily, at 10 mol % catalyst loading, linear alkyl azide **1e** is cyclized to from pyrrolidine **2e** in 40% yield (Table 2, entry 11).

I•Fe(Me) catalyst recovered from the C−H amination reaction of **1a** gave a PXRD pattern similar to that of freshly prepared **I**•Fe(Me) (Figure 1b), suggesting that the integrity of the MOF framework is maintained under reaction conditions. ICP-MS of the supernatant shows that <0.01% Fe and <0.01% Zr leached from the MOFs for **I**•Fe(Me)-catalyzed amination of **1a**. Furthermore, recovered **I**•Fe(Me) catalyst is active in a subsequent run of C−H amination reaction of **1a** (Supporting Information). At 10 mol % catalyst loading, **I**•Fe(Me) afforded **2a** in 86% yield after 24 h of reaction. **I**•Fe(Me) was recovered by centrifugation and used to catalyze the reaction a second time, affording **2a** in 90% yield while leaching 0.01% of Zr and 0.14% Fe. These results demonstrate that **I**•Fe(Me) is a highly active and reusable single-site solid catalyst giving at least 3−5 times the TONs of those of the homogeneous catalyst.

Catalytic Intermolecular C_{sp^3}−H Amination. We next sought to metalate the NacNac-MOF for the more challenging intermolecular amination of C_{sp^3}−H bonds.[29] Warren and co-workers first reported that Cu-NacNac complexes with bulky substituents enable the C_{sp^3}−H amination of a series of benzylic and cyclic alkanes utilizing tBuOOtBu as a mild oxidant.[30,31] In a related example, Hartwig and co-workers later reported Cu complexes of neutral N,N ligands catalyze the functionalization of linear and cyclic alkanes with a series of amides, benzamides, sulfonamides, and imides.[32] In both reactions, the rate-limiting step is believed to be the H atom abstraction from the aliphatic substrate.

During preliminary studies, we found that 2 mol % **I**•Cu(THF) catalyzed the reaction of aniline and cyclohexene to afford *N*-(cyclohex-2-en-1-yl)aniline in 22% yield using benzene as cosolvent (Table 3, entry 1). The yield increased to 67% when the reaction was run in neat cyclohexene (Table 3, entry 2). Notably, we did not observe the formation of diazene that is believed to occur through bimolecular reaction between two Cu-anilides.[30] Such a process cannot occur in **I**•Cu(THF) because of active site isolation in a MOF catalyst. Although only 0.09% Zr was detected in the supernatant, 7.22% Cu leached from the amination reaction, consistent with the lability of the Cu(I) center of the Cu-NacNac complex. Increasing the catalyst loading to 3 mol % gives an optimal yield of 90% (Table 3, entry 3). When the catalyst loading was reduced to 0.5 mol % and the reaction time extended to 9 days, the desired product was isolated in 75% yield (Table 3, entry 4). Homogeneous catalyst **L1**•Cu gave TONs comparable to

DOI: 10.1021/jacs.5b13394
J. Am. Chem. Soc. 2016, 138, 3501−3509

Table 3. Cu-Catalyzed Amination of Cyclohexene[a]

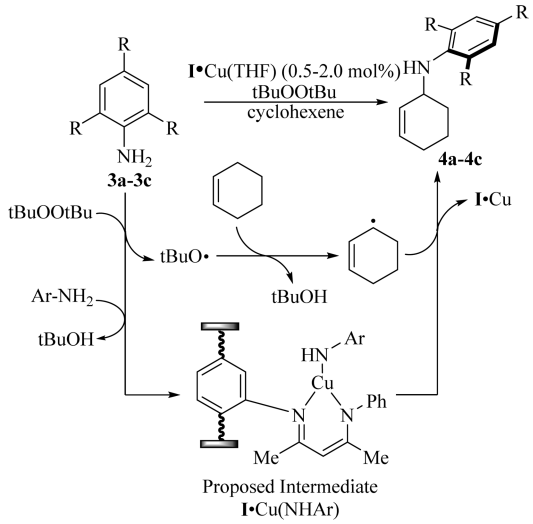

entry	catalyst (loading)	aniline (R)	yield[b]
1[c]	**I**•Cu(THF) (2)	H (**3a**)	22 (**4a**)
2	**I**•Cu(THF) (2)	H (**3a**)	67 (**4a**)
3	**I**•Cu(THF) (3)	H (**3a**)	90 (**4a**)
4[d]	**I**•Cu(THF) (0.5)	H (**3a**)	75 (**4a**)[e]
5	**I**•Fe(Me) (2)	H (**3a**)	0 (**4a**)
6	**L1**•Cu (2)	H (**3a**)	75 (**4a**)
7	**I**•Cu(THF) (2)	Me (**3b**)	61 (**4b**)
8	**L1**•Cu (2)	Me (**3b**)	90 (**4b**)
9	**I**•Cu(THF) (2)	Cl (**3c**)	38 (**4c**)
10	**L1**•Cu(2)	Cl (**3c**)	83 (**4c**)

[a]Reaction conditions: **3a**–**3c** (1 equiv), tBuOOtBu (2 equiv), cyclohexene (180 equiv), 90 °C for 2.5 days. [b]NMR yield with $MeNO_2$ as internal standard. [c]Benzene used as cosolvent with cyclohexene (30 equiv). [d]Reaction time of 9 days. [e]Isolated yield.

those of **I**•Cu(THF) under the optimized reaction conditions (Table 3, entry 2 vs 6). Finally, **I**•Fe(Me) was not active in catalyzing the intermolecular amination; the desired product was not observed from the reaction between cyclohexene and aniline at 2 mol % catalyst loading (Table 3, entry 5).

We also examined the steric and electronic influences of substituted anilines in intermolecular C–H amination reactions. In agreement with the trends observed from Warren's previous reports, homogeneous catalyst **L1**•Cu gives higher TONs for the amination with sterically congested 2,4,6-substituted anilines (Table 3, entries 8 and 10). In contrast, **I**•Cu(THF) afforded lower yields of amination products for the trisubstituted anilines **3b** and **3c**.

We followed the reaction progress for the amination of cyclohexene with either aniline (**3a**) or 2,4,6-trimethylaniline (**3b**) by GC-MS over 9 days at a reduced catalyst loading of 0.5 mol % (Figure 4). For smaller aniline **3a**, the homogeneous catalyst initially gave higher conversion than the MOF. However, the conversion afforded by **I**•Cu(THF) increased linearly, whereas the homogeneous catalyst's conversion slowed after 3 days, suggesting the decomposition of the homogeneous catalyst via bimolecular deactivation. In contrast, **L1**•Cu afforded conversions for the sterically hindered 2,4,6-trimethylaniline **3b** significantly higher than those of **I**•Cu(THF) throughout the course of the reaction, indicating the strong influence of substrate sizes due to different substrate diffusion rates. Interestingly, although 2 mol % of **L1**•Cu

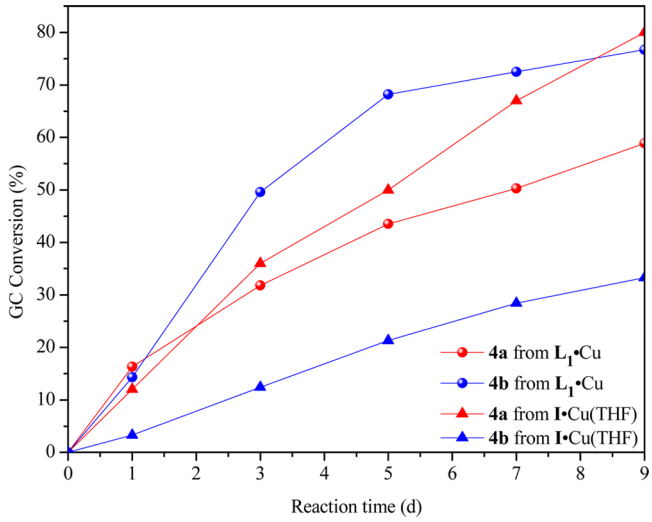

Figure 4. Plot following **L1**•Cu- and **I**•Cu(THF)-catalyzed amination of cyclohexene with either aniline (**4a**) or 2,4,6-trimethylaniline (**4b**). Reaction conditions: 0.5 mol % [Cu], 1.0 equiv of aniline (**4a** or **4b**), 2.0 equiv of tBuOOtBu, 180 equiv of cyclohexene.

catalyzed the reaction of sterically demanding 1,2,3,4-tetrahydronapthalene with aniline **3a** affording the amination product **5a** in 100% NMR yield, the MOF catalyst gave no conversion to the desired product. These results show that the MOF acts as a size-selective catalyst for the intermolecular amination reaction.

Finally, **I**•Cu(THF) could be readily recovered and reused for the amination of cyclohexene with aniline **3a** (Figure 5). At

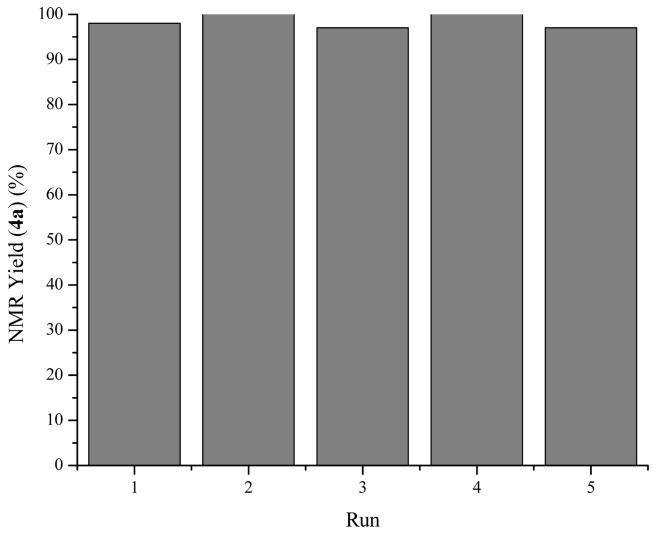

Figure 5. Plot of yield (**4a**) over consecutive runs in the recycle and reuse of **I**•Cu(THF)-catalyzed amination of cyclohexene with aniline (**3a**).

3 mol % catalyst loading, **I**•Cu(THF) was recovered and used for the amination of cyclohexene with aniline **3a** five times, giving 97–100% NMR yield each time. Even after the fifth run, PXRD studies showed that the MOF remained crystalline (Figure 1b). Taken together, the Cu-NacNac MOF **I**•Cu-(THF) is a highly active, reusable, and size-selective catalyst for intermolecular C–H amination reactions.

DOI: 10.1021/jacs.5b13394
J. Am. Chem. Soc. 2016, 138, 3501–3509

Catalytic Hydrogenation of Alkenes. Hydrogenation catalysts are widely used for the industrial production of commodity and fine chemicals and for the conversion of biomass to biorenewable fuels.[33] Historically, hydrogenation reactions are catalyzed using precious metal catalysts, but their replacement with earth-abundant first row metals is of increasing importance because of cost and availability. Homogeneous cobalt phosphine- and pyridine-based catalysts have been identified for the hydrogenation of alkenes.[34] Additionally, we recently reported a remarkable example where a homogeneous Fe-salicylaldimine complex was an inactive hydrogenation catalyst but functionalization within a MOF led to a highly active catalyst for the hydrogenation of alkenes.[4] We report here the first demonstration of catalytic hydrogenation with a Co-NacNac complex and its MOF analog.

We surveyed the catalytic activities of Co-NacNac MOFs in the hydrogenation of 1-octene. At 0.0005 mol % catalyst loading, **I**•Co(H) catalyzes the hydrogenation of 1-octene to afford *n*-octane in 100% yield in 1.5 days (Table 4, entry 1).

Table 4. Co-Catalyzed Hydrogenation of Alkenes[a]

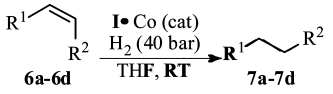

6a-6d 7a-7d

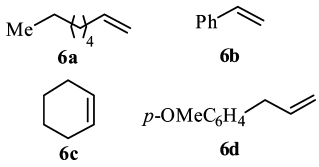

6a 6b 6c 6d

entry	substrate	catalyst (loading)	reaction time (days)	yield (%)[b]
1	**6a**	**I**•Co(H) (0.0005)	1.5	100 (97)[c]
2	**6a**	**L1**•Co(H) (0.0005)	1.5	65
3	**6a**	**L1**•Fe(H) (0.1)	1.5	10
4	**6a**	Co NP (0.0005)	1.5	6
5	**6a**	**I**•Co(H) (0.0001)	6	70
6	**6a**	**L1**•Co(H) (0.0001)	6	0
7	**6b**	**I**•Co(H) (0.0005)	1.5	100
8	**6c**	**I**•Co(H) (0.025)	3	100
9	**6d**	**I**•Co(H) (0.005)	2	79 (72)[c]

[a]Reaction conditions: H_2 (40 bar), THF (1 mL), room temperature. [b]NMR yield. [c]Isolated yield.

ICP-MS studies showed that Zr and Co were not detectable in the supernatants. For comparison, at 0.0005 mol % loading, homogeneous **L1**•Co(H) affords 65% yield of *n*-octane (Table 4, entry 2) However, **I**•Fe(H) was significantly less active, affording only 10% *n*-octane at 0.1 mol % catalyst loading (Table 4, entry 3). This result contrasts our earlier observation with the Fe-salicylaldimine MOF, which was highly active for hydrogenation of 1-octene.[4] To rule out the participation of Co nanoparticles, at 0.0005 mol % Co, only 6% conversion was observed (Table 4, entry 4). When catalyst loadings were lowered to 0.0001 mol %, **I**•Co(H) afforded *n*-octane in 70% yield, leading to a TON of 700 000 (Table 4, entry 5), whereas **L1**•Co(H) gave no conversion (Table 4, entry 6).

I•Co(H) was found to catalyze a broad scope of alkenes. Styrene (**6b**) was quantitatively hydrogenated at 0.0005 mol % of **I**•Co(H) (Table 4, entry 7). Cyclohexene was hydrogenated in quantitative yield at 0.025 mol % of **I**•Co(H) in 3 days (Table 4, entry 8). Additionally, 0.025 mol % of **I**•Co(H) catalyzed hydrogenation of 4-methoxyallylbenzene (**6d**) in 79% yield after 2 days (Table 4, entry 9).

Remarkably, at 0.005 mol % catalyst loading, **I**•Co(H) could be recovered and reused for 9 times with yields ranging from 97 to 100% (Figure 6). Isolated yields of 97 and 96% were

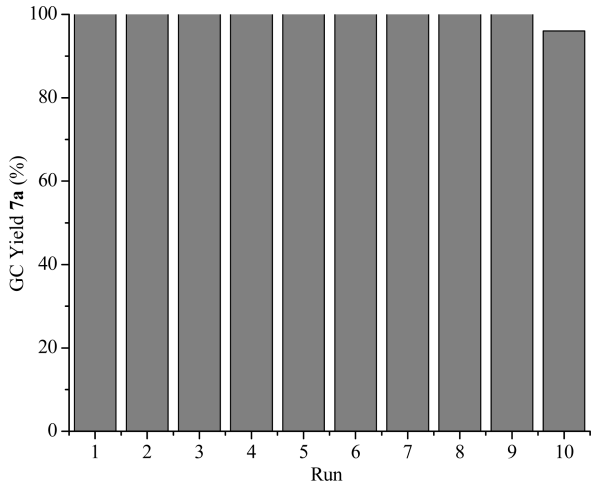

Figure 6. Plot of yield (%) of *n*-octane (**7a**) over consecutive runs in the recycle and reuse of **I**•Co(H) MOF for the hydrogenation of 1-octene.

obtained from runs 3 and 8, respectively. The Zr/Co leaching for runs 1, 2, and 7 were determined to be less than 0.01%/0.03%, 0.01%/0.01%, and 0.01%/<0.01%, respectively. After the 10th run, the crystallinity of the recovered MOF catalyst was confirmed by PXRD (Figure 1b). Altogether, the minimal metal leaching, recyclability and MOF stability demonstrate **I**•Co(H) as an excellent single-site solid catalyst for hydrogenation reactions.

CONCLUSIONS

We have developed an effective strategy for the postsynthesis installation of NacNac ligands in a porous MOF and the metalation of the NacNac moieties with Fe, Co, and Cu salts. Subsequent activation with methyl lithium, sodium triethylborohydride, or potassium tert-butoxide generated the desired MOF-immobilized monoanionic NacNac-ligated metal complexes **I**•Fe(Me), **I**•Co(H), and **I**•Cu(THF). The M-NacNac coordination environments in the MOFs were characterized by EXAFS on the basis of single-crystal X-ray structures and DFT-minimized structural models of homogeneous controls.

I•Fe(Me) catalyzed the intramolecular C_{sp^3}–H amination of alkyl azides with the highest TON reported to date. **I**•Cu was an effective catalyst for intermolecular C_{sp^3}–H amination of cyclohexene with an excellent size-selectivity. Finally, **I**•Co(H) was found to be a very effective alkene hydrogenation catalyst with TONs as high as 700 000. Importantly, the NacNac-M-MOF catalysts were more effective than their analogous homogeneous catalysts, presumably because of the active site isolation that prevents intermolecular catalyst deactivation. All of the NacNac-M-MOF catalysts could be recycled and reused without a noticeable decrease in yield and without appreciable metal leaching. PXRD studies indicated that the MOF crystallinity was retained for the catalysts recovered from the reactions. Our work thus establishes NacNac-MOFs as a novel

DOI: 10.1021/jacs.5b13394
J. Am. Chem. Soc. 2016, 138, 3501−3509

platform for engineering recyclable earth-abundant-element-based single-site solid catalysts for many important organic transformations

■ ASSOCIATED CONTENT

Supporting Information

The Supporting Information is available free of charge on the ACS Publications website at DOI: 10.1021/jacs.5b13394.

Procedures for ligand synthesis, characterization of functionalized MOFs, structural characterization of small molecule analogues, X-ray absorption spectroscopic analysis, general procedures for **I**•Fe(Me)-catalyzed amination, **I**•Cu(THF)-catalyzed amination, and **I**•Co-(H)-catalyzed hydrogenation, and NMR spectra for ligands. (PDF)

Crystallographic information file of (H−**L1**)•$CoCl_2$. (CIF)

Crystallographic information file for (H−**L1**)•$FeCl_2$. (CIF)

■ AUTHOR INFORMATION

Corresponding Author

*wenbinlin@uchicago.edu

Notes

The authors declare no competing financial interest.

■ ACKNOWLEDGMENTS

This work was supported by the National Science Foundation (NSF)(CHE-1464941). Additional support was provided by the Chicago MRSEC, which is funded by NSF through grant DMR-1420709. We thank C. Poon for help with ICP-MS analyses and Dr. Alexander S. Filatov for help with crystallographic studies. Single-crystal diffraction studies were carried out at ChemMatCARS (Sector 15), Advanced Photon Source (APS), Argonne National Laboratory (ANL). ChemMatCARS Sector 15 is principally supported by the Divisions of Chemistry (CHE) and Materials Research (DMR), NSF, under grant number NSF/CHE-1346572. XAS analysis was carried out at Beamline 9-BM, APS, ANL. Use of the APS, an Office of Science User Facility operated for the U.S. Department of Energy (DOE) Office of Science by ANL, was supported by the U.S. DOE under Contract No. DE-AC02-06CH11357.

■ REFERENCES

(1) (a) Correa, A.; Garcia Mancheno, O.; Bolm, C. *Chem. Soc. Rev.* **2008**, *37* (6), 1108−1117. (b) Bolm, C.; Legros, J.; Le Paih, J.; Zani, L. *Chem. Rev.* **2004**, *104*, 6217−6254. (c) Enthaler, S.; Junge, K.; Beller, M. *Angew. Chem., Int. Ed.* **2008**, *47*, 3317−3321. (d) Sun, C.-L.; Li, B.-J.; Shi, Z.-J. *Chem. Rev.* **2011**, *111*, 1293−1314. (e) Cahiez, G.; Moyeux, A. *Chem. Rev.* **2010**, *110*, 1435−1462. (f) Su, B.; Cao, Z. C.; Shi, Z. J. *Acc. Chem. Res.* **2015**, *48*, 886−896. (g) Holland, P. L. *Acc. Chem. Res.* **2015**, *48*, 1696−1702. (h) Gephart, R. T.; Warren, T. H. *Organometallics* **2012**, *31*, 7728−7752.

(2) Gladysz, J. A.; Bedford, R. B.; Fujita, M.; Gabbai, F. P.; Goldberg, K. I.; Holland, P. L.; Kiplinger, J. L.; Krische, M. J.; Louie, J.; Lu, C. C.; Norton, J. R.; Petrukhina, M. A.; Ren, T.; Stahl, S. S.; Tilley, T. D.; Webster, C. E.; White, M. C.; Whiteker, G. T. *Organometallics* **2014**, *33*, 1505−1527.

(3) (a) De Vos, D. E.; Dams, M.; Sels, B. F.; Jacobs, P. A. *Chem. Rev.* **2002**, *102*, 3615−3640. (b) Song, C. E.; Lee, S.-g. *Chem. Rev.* **2002**, *102*, 3495−3524. (c) Morys, P.; Schlieper, T. *J. Mol. Catal. A: Chem.* **1995**, *95*, 27−33.

(4) Manna, K.; Zhang, T.; Carboni, M.; Abney, C. W.; Lin, W. *J. Am. Chem. Soc.* **2014**, *136*, 13182−13185.

(5) (a) Gascon, J.; Corma, A.; Kapteijn, F.; Llabrés i Xamena, F. X. *ACS Catal.* **2014**, *4*, 361−378. (b) Zhao, M.; Ou, S.; Wu, C.-D. *Acc. Chem. Res.* **2014**, *47*, 1199−1207. (c) Yoon, M.; Srirambalaji, R.; Kim, K. *Chem. Rev.* **2012**, *112*, 1196−1231. (d) Falkowski, J. M.; Liu, S.; Lin, W. *Isr. J. Chem.* **2012**, *52*, 591−603. (e) Ma, L.; Abney, C.; Lin, W. *Chem. Soc. Rev.* **2009**, *38*, 1248−1256. (f) Lee, J. Y.; Farha, O. K.; Roberts, J.; Scheidt, K. A.; Nguyen, S. B. T.; Hupp, J. T. *Chem. Soc. Rev.* **2009**, *38*, 1450−1459.

(6) Manna, K.; Zhang, T.; Greene, F. X.; Lin, W. *J. Am. Chem. Soc.* **2015**, *137*, 2665−2673.

(7) (a) Manna, K.; Zhang, T.; Lin, W. *J. Am. Chem. Soc.* **2014**, *136*, 6566−6569. (b) Fei, H.; Cohen, S. M. *Chem. Commun.* **2014**, *50*, 4810−4812. (c) Falkowski, J. M.; Sawano, T.; Zhang, T.; Tsun, G.; Chen, Y.; Lockard, J. V.; Lin, W. *J. Am. Chem. Soc.* **2014**, *136*, 5213−5216. (d) Sawano, T.; Thacker, N. C.; Lin, Z.; McIsaac, A. R.; Lin, W. *J. Am. Chem. Soc.* **2015**, *137*, 12241−12248. (e) Mo, K.; Yang, Y.; Cui, Y. *J. Am. Chem. Soc.* **2014**, *136*, 1746−1749. (f) Genna, D. T.; Wong-Foy, A. G.; Matzger, A. J.; Sanford, M. S. *J. Am. Chem. Soc.* **2013**, *135*, 10586−10589. (g) Zhu, C.; Yuan, G.; Chen, X.; Yang, Z.; Cui, Y. *J. Am. Chem. Soc.* **2012**, *134*, 8058−8061. (h) Kong, G.-Q.; Ou, S.; Zou, C.; Wu, C.-D. *J. Am. Chem. Soc.* **2012**, *134*, 19851−19857. (i) Zheng, M.; Liu, Y.; Wang, C.; Liu, S.; Lin, W. *Chem. Sci.* **2012**, *3*, 2623−2627. (j) Wang, C.; Wang, J.-L.; Lin, W. *J. Am. Chem. Soc.* **2012**, *134*, 19895−19908. (k) Fateeva, A.; Chater, P. A.; Ireland, C. P.; Tahir, A. A.; Khimyak, Y. Z.; Wiper, P. V.; Darwent, J. R.; Rosseinsky, M. J. *Angew. Chem., Int. Ed.* **2012**, *51*, 7440−7444. (l) Sawano, T.; Ji, P.; McIsaac, A. R.; Lin, Z.; Abney, C. W.; Lin, W. *Chem. Sci.* **2015**, *6*, 7163−7168.

(8) (a) He, C.; Liu, D.; Lin, W. *Chem. Rev.* **2015**, *115*, 11079−11108. (b) Horcajada, P.; Gref, R.; Baati, T.; Allan, P. K.; Maurin, G.; Couvreur, P.; Ferey, G.; Morris, R. E.; Serre, C. *Chem. Rev.* **2012**, *112*, 1232−1268. (c) Della Rocca, J.; Liu, D.; Lin, W. *Acc. Chem. Res.* **2011**, *44*, 957−968. (d) Huxford, R. C.; Della Rocca, J.; Lin, W. *Curr. Opin. Chem. Biol.* **2010**, *14*, 262−268.

(9) (a) Wang, C.; Zhang, T.; Lin, W. *Chem. Rev.* **2012**, *112*, 1084−1104. (b) Evans, O. R.; Lin, W. *Acc. Chem. Res.* **2002**, *35*, 511−522.

(10) (a) Carboni, M.; Abney, C. W.; Liu, S.; Lin, W. *Chem. Sci.* **2013**, *4*, 2396−2402. (b) Yee, K. − K.; Reimer, N.; Liu, J.; Cheng, S. − Y.; Yiu, S. − M.; Weber, J.; Stock, N.; Xu, Z. *J. Am. Chem. Soc.* **2013**, *135*, 7795−7798.

(11) (a) Suh, M. P.; Park, H. J.; Prasad, T. K.; Lim, D.-W. *Chem. Rev.* **2012**, *112*, 782−835. (b) Sumida, K.; Rogow, D. L.; Mason, J. A.; McDonald, T. M.; Bloch, E. D.; Herm, Z. R.; Bae, T.-H.; Long, J. R. *Chem. Rev.* **2012**, *112*, 724−781. (c) Dinca, M.; Long, J. R. *Angew. Chem., Int. Ed.* **2008**, *47*, 6766−6779. (d) Rowsell, J. L. C.; Yaghi, O. M. *Angew. Chem., Int. Ed.* **2005**, *44*, 4670−4679.

(12) (a) Cavka, J. H.; Jakobsen, S.; Olsbye, U.; Guillou, N.; Lamberti, C.; Bordiga, S.; Lillerud, K. P. *J. Am. Chem. Soc.* **2008**, *130*, 13850−13851. (b) Kandiah, M.; Nilsen, M. H.; Usseglio, S.; Jakobsen, S.; Olsbye, U.; Tilset, M.; Larabi, C.; Quadrelli, E. A.; Bonino, F.; Lillerud, K. P. *Chem. Mater.* **2010**, *22*, 6632−6640.

(13) (a) Chen, C.; Bellows, S. M.; Holland, P. L. *Dalton Trans.* **2015**, *44*, 16654−16670. (b) Tsai, Y.-C. *Coord. Chem. Rev.* **2012**, *256*, 722−758. (c) Bourget-Merle, L.; Lappert, M. F.; Severn, J. R. *Chem. Rev.* **2002**, *102*, 3031−3066.

(14) Roesler, S.; Obenauf, J.; Kempe, R. *J. Am. Chem. Soc.* **2015**, *137*, 7998−8001.

(15) Holland, P. L.; Cundari, T. R.; Perez, L. L.; Eckert, N. A.; Lachicotte, R. J. *J. Am. Chem. Soc.* **2002**, *124*, 14416−14424.

(16) Hili, R.; Yudin, A. K. *Nat. Chem. Biol.* **2006**, *2*, 284−287.

(17) Louillat, M.-L.; Patureau, F. W. *Chem. Soc. Rev.* **2014**, *43*, 901−910.

(18) Ritchie, T. J.; MacDonald, S. J. F.; Young, R. J.; Pickett, S. D. *Drug Discovery Today* **2011**, *16*, 164−171.

(19) (a) Kienle, M.; Reddy Dubbaka, S.; Brade, K.; Knochel, P. *Eur. J. Org. Chem.* **2007**, *2007*, 4166−4176. (b) Takemoto, Y.; Miyabe, H. *Compr. Organomet. Chem. III* **2007**, *10*, 695−724.

DOI: 10.1021/jacs.5b13394
J. Am. Chem. Soc. 2016, 138, 3501−3509

(20) Vo, C.-V. T.; Bode, J. W. *J. Org. Chem.* **2014**, *79*, 2809−2815.
(21) Klapars, A.; Campos, K. R.; Waldman, J. H.; Zewge, D.; Dormer, P. G.; Chen, C.-y. *J. Org. Chem.* **2008**, *73*, 4986−4993.
(22) Lloyd, J.; Finlay, H. J.; Vacarro, W.; Hyunh, T.; Kover, A.; Bhandaru, R.; Yan, L.; Atwal, K.; Conder, M. L.; Jenkins-West, T.; Shi, H.; Huang, C.; Li, D.; Sun, H.; Levesque, P. *Bioorg. Med. Chem. Lett.* **2010**, *20*, 1436−1439.
(23) Campos, K. R. *Chem. Soc. Rev.* **2007**, *36*, 1069−1084.
(24) Hennessy, E. T.; Betley, T. A. *Science* **2013**, *340*, 591−595.
(25) Broere, D. L. J.; de Bruin, B.; Reek, J. N. H.; Lutz, M.; Dechert, S.; van der Vlugt, J. I. *J. Am. Chem. Soc.* **2014**, *136*, 11574−11577.
(26) (a) Cowley, R. E.; Holland, P. L. *Inorg. Chem.* **2012**, *51*, 8352−8361. (b) Cowley, R. E.; Eckert, N. A.; Vaddadi, S.; Figg, T. M.; Cundari, T. R.; Holland, P. L. *J. Am. Chem. Soc.* **2011**, *133*, 9796−9811. (c) Cowley, R. E.; Eckert, N. A.; Elhaik, J.; Holland, P. L. *Chem. Commun.* **2009**, 1760−1762.
(27) (a) Bollinger, J. M., Jr.; Price, J. C.; Hoffart, L. M.; Barr, E. W.; Krebs, C. *Eur. J. Inorg. Chem.* **2005**, *2005*, 4245−4254. (b) Price, J. C.; Barr, E. W.; Tirupati, B.; Bollinger, J. M., Jr.; Krebs, C. *Biochemistry* **2003**, *42*, 7497−7508.
(28) Cowley, R. E.; Elhaik, J.; Eckert, N. A.; Brennessel, W. W.; Bill, E.; Holland, P. L. *J. Am. Chem. Soc.* **2008**, *130*, 6074−6075.
(29) Roizen, J. L.; Harvey, M. E.; Du Bois, J. *Acc. Chem. Res.* **2012**, *45*, 911−922.
(30) Gephart, R. T.; Huang, D. L.; Aguila, M. J. B.; Schmidt, G.; Shahu, A.; Warren, T. H. *Angew. Chem., Int. Ed.* **2012**, *51*, 6488−6492.
(31) (a) Gephart, R. T.; Warren, T. H. *Organometallics* **2012**, *31*, 7728−7752. (b) Jang, E. S.; McMullin, C. L.; Kass, M.; Meyer, K.; Cundari, T. R.; Warren, T. H. *J. Am. Chem. Soc.* **2014**, *136*, 10930−10940. (c) Wiese, S.; Badiei, Y. M.; Gephart, R. T.; Mossin, S.; Varonka, M. S.; Melzer, M. M.; Meyer, K.; Cundari, T. R.; Warren, T. H. *Angew. Chem., Int. Ed.* **2010**, *49*, 8850−8855.
(32) Tran, B. L.; Li, B.; Driess, M.; Hartwig, J. F. *J. Am. Chem. Soc.* **2014**, *136*, 2555−2563.
(33) (a) Corma, A.; Iborra, S.; Velty, A. *Chem. Rev. (Washington, DC, U. S.)* **2007**, *107*, 2411−2502. (b) de Vries, J. G., Elsevier, C. J., Eds. *The Handbook of Homogeneous Hydrogenation*; Wiley-VCH: Weinheim, Germany, 2007.
(34) (a) Friedfeld, M. R.; Margulieux, G. W.; Schaefer, B. A.; Chirik, P. J. *J. Am. Chem. Soc.* **2014**, *136*, 13178−13181. (b) Friedfeld, M. R.; Shevlin, M.; Hoyt, J. M.; Krska, S. W.; Tudge, M. T.; Chirik, P. J. *Science* **2013**, *342*, 1076−1080. (c) Yu, R. P.; Darmon, J. M.; Milsmann, C.; Margulieux, G. W.; Stieber, S. C. E.; DeBeer, S.; Chirik, P. J. *J. Am. Chem. Soc.* **2013**, *135*, 13168−13184. (d) Monfette, S.; Turner, Z. R.; Semproni, S. P.; Chirik, P. J. *J. Am. Chem. Soc.* **2012**, *134*, 4561−4564. (e) Knijnenburg, Q.; Horton, A. D.; van der Heijden, H.; Kooistra, T. M.; Hetterscheid, D. G. H.; Smits, J. M. M.; de Bruin, B.; Budzelaar, P. H. M.; Gal, A. W. *J. Mol. Catal. A: Chem.* **2005**, *232*, 151−159. (f) Zhang, G.; Scott, B. L.; Hanson, S. K. *Angew. Chem., Int. Ed.* **2012**, *51*, 12102−12106.

DOI: 10.1021/jacs.5b13394
J. Am. Chem. Soc. 2016, 138, 3501−3509